Effect of Buffer Layer on Interface Bond Strength and Abrasive Wear of Hard Faced Cast Iron

Nirmal Saha and Tapan Kumar Pal

Welding Technology Centre, Metallurgical and Material Engineering Department, Jadavpur University, Kolkata-700032.
Email : tkpal.ju@gmail.com

ABSTRACT

The effect of five different buffer layers followed by a hardfacing electrode deposited on gray cast iron plate (ASTM grade 2500) upon performance of interface between substrate cast iron and deposited layers as well as abrasive wear behaviour of hardfaced deposits were studied. The results show that high nickel buffer electrode attributed best performance of interface bond in terms of shear strength and relatively lower nickel buffer electrode attributed best abrasive wear properties. The shear strength at the interfaces and wear properties has been correlated with microstructure and micro-mechanism of fracture in shear strain and micro-mechanism of metal removal in abrasive wear.

Keywords: Buffer layer, Hardfacing, Hardness, Carbides, Bond strength, Abrasive wear

1.0 INTRODUCTION

Wear is the leading cause for many components worn-out in service, causing a great deal of scrap metal and economic loss in production. Although surface coatings can be applied in verity of ways, in heavy engineering, welding is still the principal method of protecting the surfaces of engineering components that are subjected to some form of attack in service. In particular engineering situations, preparation of hardfacing deposits requires selection of welding consumables and procedure for a given welding process. Manual metal arc welding process is most commonly used because reasonably rapid work of In-situ repair can be carried out without specialized equipment and only with moderate degree of skill.

Present investigation was carried out with thermal power plant component called top bearing plate, which is made up of ASTM grade 2500 gray cast iron, suffers from wear due to rubbing action of uncrushed coal particles. The worn cast iron part was practiced to rebuilt first with nickel based buffer layer followed by weld deposits with commercially available hardfacing electrode. However, the life of such hardfacing deposit was not satisfactory and the application of nickel base buffer electrode made the rebuilding process more costly. Based on the above industrial problem hardfacing electrode with improved life was developed and detail study on the microstructure and wear properties of hardfacing deposits using developed electrode and commercially available hardfacing electrode was reported [1].

To minimize performance losses of hardfacing deposits due to dilution, particularly in case of brittle substrate such as cast iron, it is often necessary to employ a buffer layer, usually high nickel content, followed by hard layer. In actual practice, a number of buffer electrodes for cast iron are commercially available, based largely on nickel-iron, nickel-copper alloys. However, there are no simple laws governing the selection of buffer electrode for hardfacing cast iron. In order to select suitable buffer electrode from technical as well as economical point of view, it is therefore necessary to understand the effect of different buffer layer on overall performance of hardfacing

deposits. Again, the application of different buffer layers on the performance of hardfacing deposits on top bearing plate was not studied in detail.

In the present study, four different buffer electrodes with varying nickel content and one buffer electrode containing copper in addition to nickel (monel type) were first deposited on cast iron followed by a developed hardfacing electrode containing niobium and molybdenum along with chromium and carbon. The aim of the study is to evaluate the effect of different buffer electrodes on bond strength between substrate and hardfacing deposits and wear properties of hardfacing deposits (double layer).

2.0 EXPERIMENTAL

2.1 Materials

The substrate material was sand mould casted gray cast iron plate (ASTM grade 2500) with dimensions of 90mm x 85mm x 20mm. Hardfacing was performed upon this gray cast iron substrate plates using five different types of buffer alloys followed by one developed hardfacing tubular wire.

2.2 Welding Conditions

Before welding the electrodes were dried at 100^{0}C for 2 hrs. Preheat was applied by placing the test block in a furnace at 400^{0}C and was maintained as an inter-pass temperature for deposition of adjacent beads. On completion of weld deposits, each test piece was allowed to cool in air.

Single layer of buffer deposits consisted of 15 beads with approximately 25% overlap between each and single layer of hardfacing deposits consisted of 9 beads with approximately 25% overlap between each bead. Preparations of test specimen for evaluation of bond strength, welding were done across the thickness side of cast iron followed by same welding parameters and procedure. The welding parameters of the hardfacing electrodes and buffer electrodes are given in **Table 1.**

2.3 Chemical composition, Metallography and Hardness test

Chemical compositions of gray cast iron base plates, buffer and hardfacing electrodes deposited on water cooled copper plates were determined by weight chemical analysis (**Table.2 to 4**). Hardfacing deposited plates were sectioned for deposit chemistry, metallography samples and hardness test. The deposit chemistry (**Table 5**) was also determined by weight chemical analysis after collecting the thin slice of about 1.5 mm thickness from the top of each hardface deposited plate with the help of diamond (ISO MET) cutter.

Metallography test samples were then ground, polished and etched with Villella's reagent (one part HNO_3, two parts HCl and three parts Glycerol) to develop the microstructures of the top surfaces. The microstructures were observed using both an optical and scanning electron microscope (SEM). Different types of carbide present in the microstructure were first identified on the basis of their morphologies as observed by other investigators [2, 3]. Later the types of those carbides were confirmed by Energy Dispersive X-Ray Spectroscopy (EDX) followed by taking micro-hardness. Microstructures of the interface regions were performed on the transverse section of the hardfacing deposits using 2% nital to reveal micro-structure of cast iron substrate and Villella's reagent to reveal microstructure of nickel buffer and hardface layer.

Bulk hardness values of different hardface deposits were taken in a Vicker's hardness testing m/c using 30kg and a 136^0 diamond pyramid indenter. Hardness of the deposit layers was determined by using the average of five measurements taken on the surface. Knoop micro-hardness survey was made across the hardface deposited plates starting from cast iron substrate to top of the hardface layer at an interval of 0.4mm using 0.5 kgf load.

Table 1: Welding Parameters

Electrode	Average Current (A)	Average Voltage (V)	Average Speed (mm/s)	Heat input (kJ/mm)
Buffer Ellectrode	150	25	2.25	1.333
Hardfacing Electrode	135	30	2.2	1.440

Table 2 : Chemical composition of base metal

Material	%C	%Mn	%Si	%Ni	%Cr	%Nb	%Mo	%S	%P	%Fe
BM	3.23	0.61	1.83	---	---	---	---	0.096	0.256	Rest

Table 3 : Chemical composition of the buffer electrodes

Buffer	%Ni	%Cu	%Fe
B1	32.85	---	Rest
B2	36.5	---	Rest
B3	39.92	---	Rest
B4	56.57	21.45	Rest
B5	88.2	---	Rest

Table 4 : Chemical composition of the hardfacing electrodes

Material	%C	%Mn	%Si	%Ni	%Mo	%Cr	%Nb	%Fe
Hardfacing electrode	4.74	0.9	0.5	1.73	2.2	19.89	6.58	Rest

Table 5 : Chemical composition of the Hardfacing deposits

Sample	%C	%Mn	%Si	%Ni	%Mo	%Cr	%Nb	%Fe
D1	3.28	0.72	0.81	9.03	0.9	10.12	3.1	Rest
D2	3.80	0.77	0.79	6.83	1.3	12.83	3.8	Rest
D3	3.74	0.81	0.95	11.16	1.6	14.31	3.91	Rest
D4	3.72	0.70	0.80	11.79	1.7	13.65	3.8	Rest
D5	3.70	0.71	0.75	15.50	1.5	12.8	3.74	Rest

2.4 Bond Strength

Bond Strength between the substrate and weld deposits of each sample was evaluated in a hydraulic press using a specially design fixture. A shear force was applied along the bond region between substrate and a buffer/hardface layer. Test sample as per the dimension was fitted in the sample holder in such a way that the welded portion of the sample remains outside the holder. Then the sample holder was fitted in the guide so that the ram just touches the hardface portion of the sample. The ram and sample holder containing the sample was fitted within a hydraulic press. A load cell was kept in series along the centre line of the fixture in order to measure the applied load. A compressive load was applied to fixture through the hydraulic press. As a result the sample within the fixture experienced a shear stress across the bond line and the sample ultimately failed at the bond region with the progressive increase in shear stress. The load at which each sample failed across the bond line was recorded and bond strength was calculated based on the maximum load divided by respective cross sectional area at the fracture surface. The shear fracture surfaces were observed under SEM to understand the micro-mechanism of such failure.

2.5 Abrasive Wear Test

Before the abrasive wear test all the specimens were cleaned with acetone and then weighed on an electronic balance with an accuracy of ±0.1 mg. The Wear testing of different hardface deposited samples was conducted using an ASTM G-65 dry sand/rubber wheel abrasive testing m/c. Rounded quartz grain sand was used as abrasive particle of sizes 50-70 mesh. The sands were baked at 150^{0}C in a furnace for one hour and then cooled to room temperature before the test. The testing parameters were: load 13.5 kg, sand flow rate 250 g/min, wheel rotation 200 rpm, wheel diameter 228.6 mm and total revolution of the wheel was 2000 for each test. After each test the specimen was cleaned with acetone and then weighed on the electronic balance. Weighed loss data was recorded for each sample.

2.6 Wear surface study

The wear specimens were washed with care by acetone to avoid the destruction of worn surface. Then the worn surfaces were observed under SEM to characterize the surface morphology and to establish possible mechanism for material removal.

3.0 RESULTS AND DISCUSSION

Main objective of the present investigation was to study the effect of different types of buffer electrodes upon the performance of interface between substrate cast iron and hardfacing deposits and abrasive wear resistance of hardfacing deposits. To explore the performance of such interface i.e. between substrate cast iron and buffer/hardfacing layer, the shear strength of hardfacing deposited sample at their respective interfaces were evaluated. Since there is no standard method for evaluating the performance of such interface, shear strength values at their interfaces have been considered and compared among different weld deposits made with different buffer layers. Furthermore, microstructures and hardness survey in the transverse section of the weld deposits have been made to understand the interface shear strength.

3.1 Bond Strength

Microstructure of sample using high nickel buffer layer showed fully austenitic matrix with some graphite nodules (Fig. 1(a)). Such graphite nodule is not unexpected considering the migration of more amounts of carbon and silicon from cast iron substrate into the nickel buffer and transformation of carbon into graphite in nodular form due to presence of high nickel and silicon. Furthermore, absence of carbides in the microstructure probably indicates that excess carbon, if any, has been dissolved in austenite. Microstructures of weld deposits with low nickel buffer electrodes however, consist of network of cementite in a pearlitic matrix (**Fig.1 (b)**). Such microstructure is expected considering the dilution of the substrate gray cast iron with low nickel buffer electrode forming deposition with composition close to hyper-eutectoid steel. Such microstructural change across the interface of different weld deposits is quite evident from the microhardness (knoop) profile as shown in **Fig 2 (a). Fig.2 (a)** also reveals that with increasing nickel content in buffer layer hardness decreases. A transition zone is observed in the hardness profile between substrate and hardface with buffer layers. Shear strength between substrate and buffer layers as shown in Fig. 2 (b) reveals that low nickel base buffer layers such as D1, D2, D3, have comparatively low shear strength compare to high nickel base buffer layers (D4, D5). Although, among the low nickel base buffer layers D3 has the lowest shear strength and between the high nickel base buffer layers D5 has the highest shear strength.

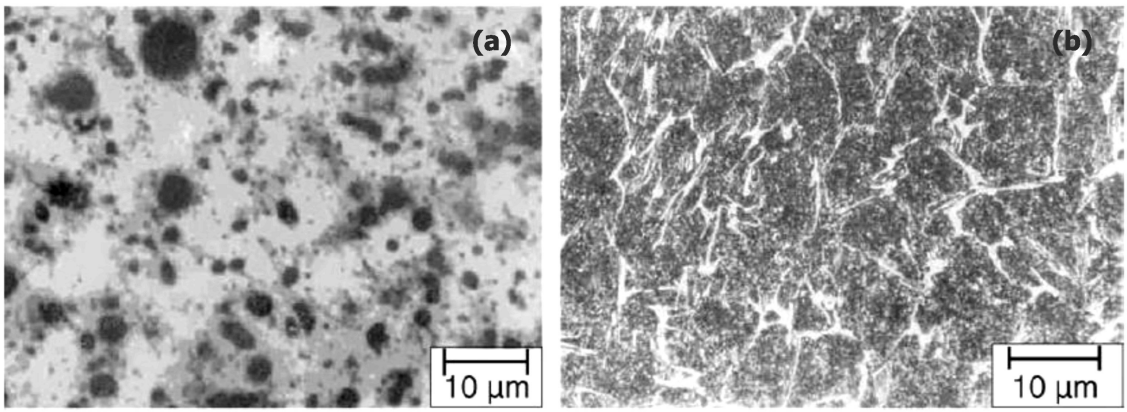

Fig. 1 : Microstructure of different interfaces using different buffer layers (a) high Ni and (b) low Ni

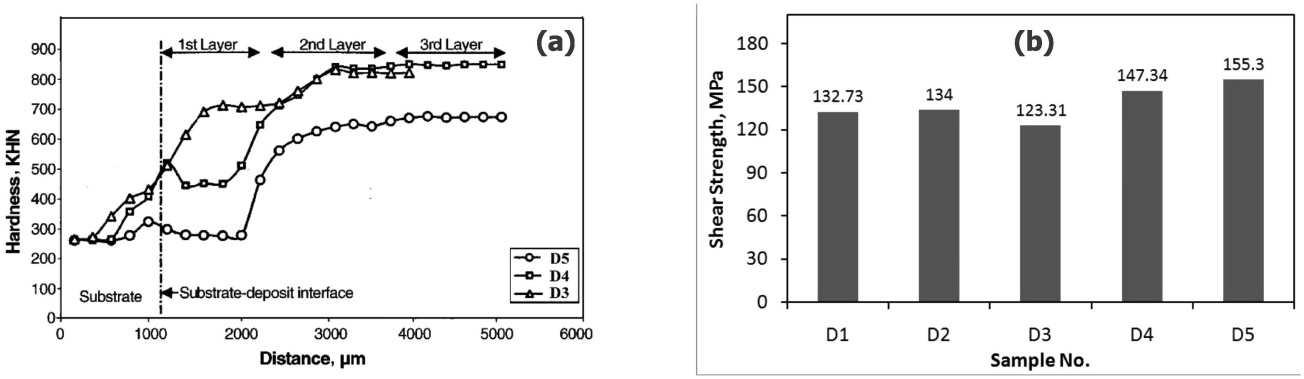

Fig. 2 : (a) Micro hardness profile taken across the weld deposits and (b) Shear strength of different weld deposits; using different Ni buffers

The results of the shear strength between substrate and buffer layers may be explained by considering the micro-mechanism involved in shear fracture. Shear fracture involves the initiation of voids and its growth in the tri-axial stress field. On application of strain, a plastic zone is produced and as the strain is increased, cavities initiates around the graphite/ carbides in the matrix. At the microstructure level, the increase in strength may be visualized as an increase in the dislocation density tangled around second phase particles. The dislocation exerts stress on the particle and on the particle/ matrix interface and as a result the particle may fracture, shear or decohese from the matrix. The factors which affect these initiation strengths are segregation of impurities to particle/ matrix interfaces, chemical composition of the particle, particle shape, dislocation concentration of the matrix and ability of the matrix to work harden [4].

It follows that area fraction of voids observed on the fracture surface as shown in **Fig 3** can indicate bond strength. In nickel buffer specimen, the area fraction is large (**Fig. 3 (a)**), indicating that the large voids have grown to substantial sizes prior to shear linkage i.e. the inter void strains are large indicating higher bond strength. On the other hand, in low nickel buffer specimens the area fractions of void is smaller (**Fig. 3 (b)**) and hence less inter void strain is required to initiate the "shear linkage" which is likely to possess lower bond strength [5]. Furthermore, the ability of the matrix to work harden is expected to be more in high nickel base buffer layer with austenitic matrix (**Fig.3 (a)**) as compared to other low nickel buffer layer. These two factors probably responsible for improved shear strength associated with high nickel base buffer layer as compared to other low nickel buffer layer.

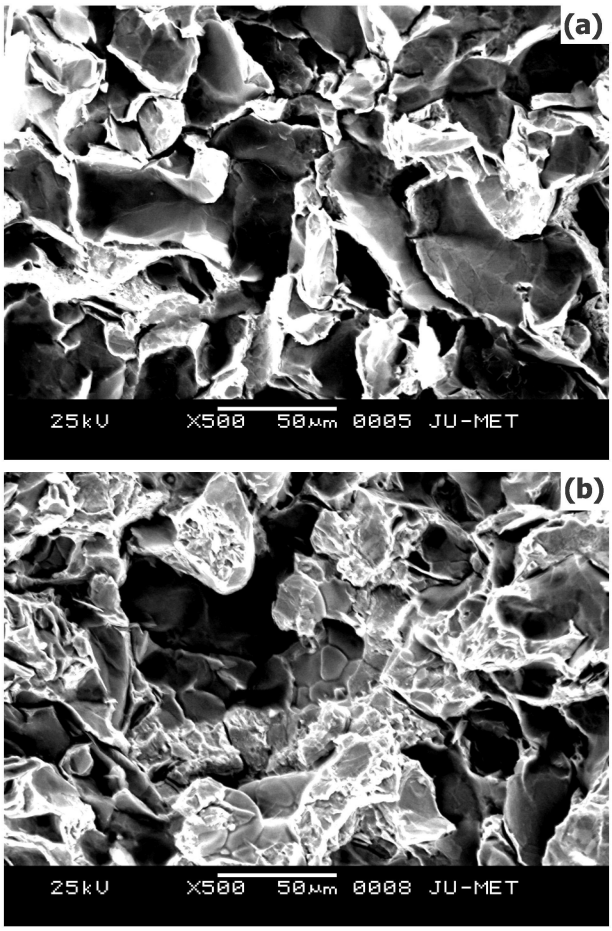

Fig. 3: Scanning electron micrographs of fractured bond regions using (a) buffer electrode B5 and (b) buffer electrode B3

3.2 Abrasive Wear

Abrasive wear data in terms of mass loss and corresponding average hardness values are given in **Table 6**. Significant differences in wear rate exist among the five weld hardfacing deposits. Maximum wear rate occurred in hardfaced deposits using buffer electrode type B1. While hardfaced deposits using buffer electrode type B3 showed lowest wear rate under low stress abrasion test.

For a given wear system the microstructure of weld deposits plays a strong role in influencing the wear resistance. Microstructures of hardfaced deposited samples using different buffer electrodes are shown in **Fig. 4**. The Fe-Cr-C system (**Fig. 5**) [6] suggests that solidification of hardfacing deposits used begin with the formation of primary M_7C_3 carbides. After primary solidification of hard phases, the melt could remain hypo-eutectic or eutectic. During the hypo-eutectic solidification first the metal matrix solidifies as metal cells they were surrounded by eutectic. If the remaining melt had a eutectic composition, the eutectic would surround the primary coarse hard phases directly. Thus eutectic always solidified in the shape of network which is observed in single layer of hardfacing deposit (**Fig. 6 (a)**). According to the structure of eutectic hard phases the eutectic was lamellar or skeletal. The layer deposited first (single hardfacing layer) is diluted heavily by mixing with the cast iron base plate, so that it's microstructure was found to consist largely of primary austenite dendrites (**Fig. 6 (b)**) instead of primary M_7C_3. By adding niobium the volume fraction of hard phases increases due to the additional solidification of the mono-carbides of these elements [7]. In fact, microstructures of all the weld hardfaced deposits show niobium (N_b) carbides (**Fig. 7**). The presence of N_b in the carbides along with Cr can be evident from EDX analysis as shown in **Fig. 8**. This is due to the fact that niobium was partitioned neither to MC nor to M_7C_3, but it is preferentially partitioned to primary and eutectic N_bC. Furthermore, niobium being a strong carbide former form earlier and acts as nucleation sites for chromium carbides to precipitate [8].

Many factors such as carbide type and hardness, volume fraction, orientation and the mean free path of the material between carbides affect the abrasion resistance. Harder carbide types have been shown to improve the abrasion resistance [9]. Cr_7C_3 is much harder (approx. 2100 DPH) than Fe_3C (approx. 1300 DPH) [10] and would therefore be expected to show better wear resistance. Niobium carbide having hardness approx. 2400Hv will contribute wear resistance in a similar manner. However, variation in hardness values of hard phases is not unlikely as mono-carbides can solidify with different stoichiometric compositions [7], a fact which influences their lattice constants and hardness [11]. Also, the carbides of M_7C_3 type dissolve different amounts of Cr depending on the temperature of solidification, but the carbon content stays about the same [7]. Additionally, hardness of all hard phases depends on the orientation of the lattice in respect to the indentation [12]. Under low stress abrasion conditions several researchers have found that increasing the carbide volume fraction improves the abrasion resistance [13, 14, 15]. In the present investigation, the carbide volume fraction as calculated from the equation (1) [7] is shown in **Fig. 9**. It appears that there is not much variation in carbide volume fraction among the different hardfaced samples except sample D1which shows less volume fraction of carbides.

$$\%CV = 12.33(\%C) + 0.55(\%Cr) - 15.2 \quad (1)$$

It is well established that the influence of the matrix on abrasive wear performance is related to the degree of protection offered by the carbides. If the carbides protect the matrix from the abrasive particles, role of matrix is merely to provide mechanical support. However, if the matrix is not protected, and is preferentially removed by the abrasion process, the carbides may become unsupported and susceptible to spalling and fracture. Under these conditions, the abrasion resistance of the matrix is critical as this controls the rate at which the carbides become unsupported and fracture. A martensitic matrix improves the low stress abrasion resistance [16, 17] by reducing the wear of the matrix and hence the rate at which carbides fractured. Although a metastable austenite matrix is commonly retained in the ambient temperature [18], a fully austenitic matrix retained to room temperature when Ms is below room temperature and sufficient alloying elements are added to avoid martensite [19]. Furthermore, as the Cr content increases the range of carbon contents that will produce an austenitic matrix at room temperature increases [20]. However, the majority of Cr is combined with carbon in the carbides and therefore the Cr content in the matrix is quite low [21]. In order to achieve sufficient hardenability, Mo, Ni, Mn etc are commonly added [22, 23]. Ni and Cu are found exclusively in the matrix region [24], while Mn may partly segregate to the carbides, reducing its effectiveness. Si on the other hand decreases the solubility of carbon in austenite and hence the carbon content in the matrix. Further, Si addition gives an increase in the Ms-temperature. While most elements tend to decrease the Ms-temperature [13], Mo, however, has little effect on Ms-temperature. On the basis of above discussion it could be predicted that presence of higher Cr and Si in the hardfaced deposits using buffer electrode type B3 may produce martensite in the matrix. This is not unexpected considering its hardness value of 621 Hv which is within the regime of martensite matrix as reported by previous investigator [7]. Additions of Ni, Mn and Cu have been considered detrimental to wear resistance possibly due to over stabilisation of the austenite within the higher alloy content [25, 26].

In view of the fore going, the hardfacing deposits with buffer electrode D3 type is expected to attribute improved wear resistance due to favourable microstructure i.e. hard carbides in a matrix of mostly austenite and some amount of martensite which will better control the extent to which the carbide became exposed and fracture. On the other hand, the hardfacing deposits with other buffer electrode types containing hard carbides in austenitic matrix are expected to provide less protection of the carbides leading to poor wear resistance. However, variation in wear rate even with austenitic matrix could be due to little variation in volume fraction of carbides and toughness of the matrix [16] which is probably controlled by the presence of Cr and Ni in austenite. Accordingly, the lower abrasive wear resistance of sample D1 is expected considering the presence of lower amounts of carbides and less tougher austenitic matrix.

Examination of wear scars that the damage morphologies for all the samples were similar, consisting of three zones, a short entrance and exit area and the main wear zone in middle. In the centre of wear scar, parallel grooves were formed, typical of particle sliding, a results of the higher pressures forcing abrasives into rubber wheel. The worn surfaces are characterized by shallow continuous grooves and micro-cutting (**Fig. 10**) in samples indicating that material removal is associated primarily with ploughing mechanisms.

Table 6 : Mass loss due to abrasive wear and corresponding average hardness values of different samples

Sample No.	Avg. Mass loss (g)	Avg. Hardness (VHN)
D1	0.5707	564
D2	0.3091	566
D3	0.2843	621
D4	0.3916	499
D5	0.4748	509

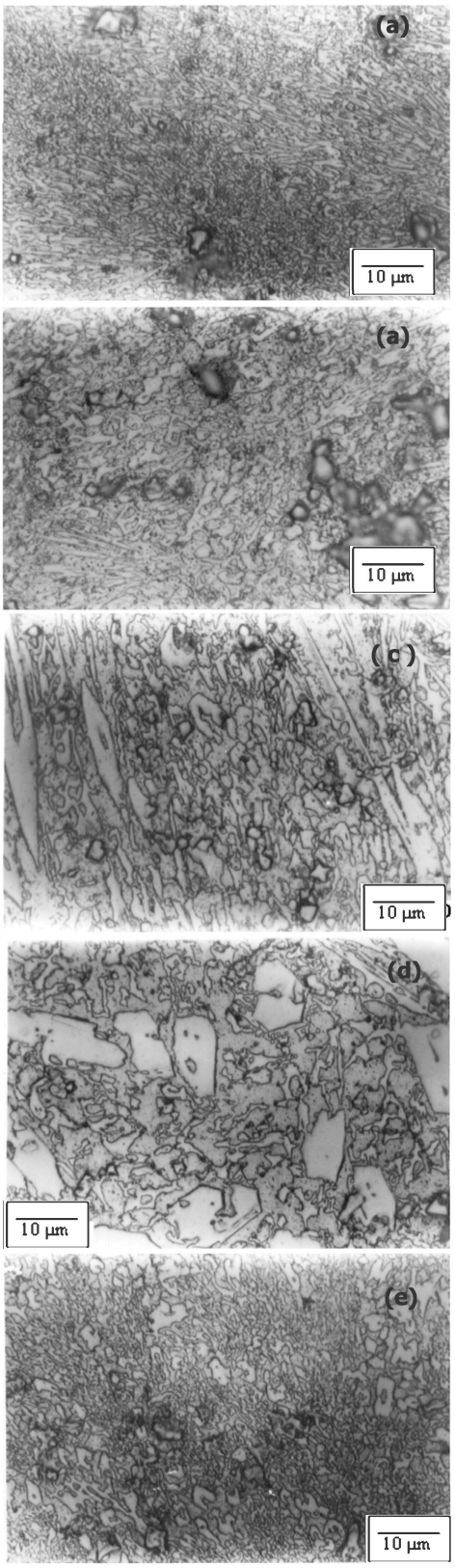

Fig. 4 : Microstructure of different samples (a) sample D1, (b) sample D2, (c) sample D3, (d) sample D4 and (e) sample D5

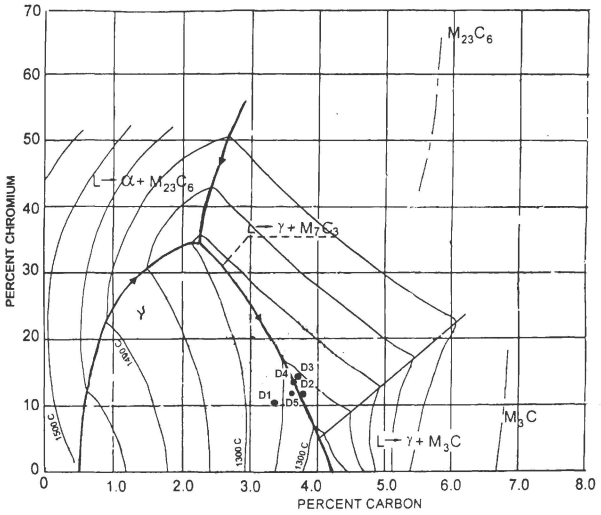

Fig. 5 : Fe-Cr-C phase diagram showing the positions of different hardfacing deposits

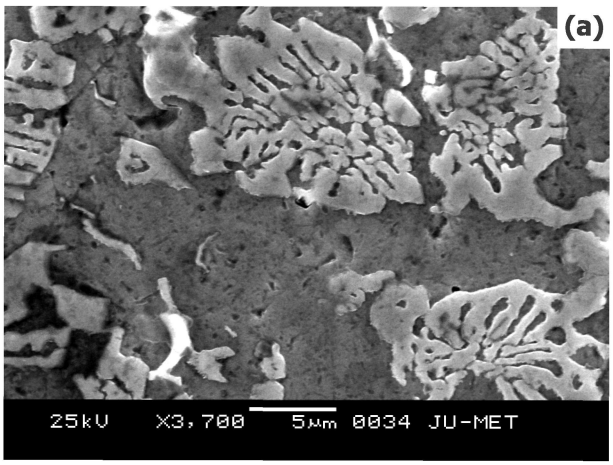

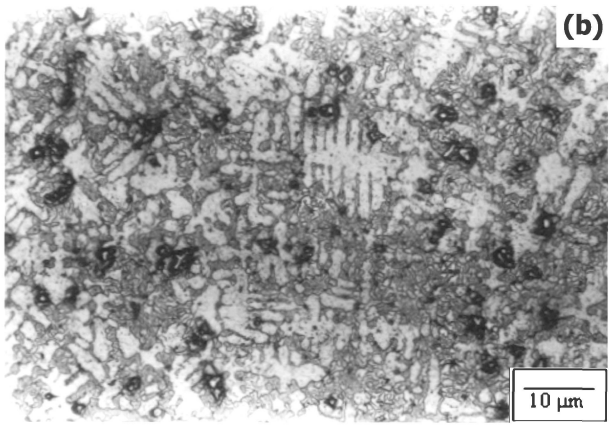

Fig. 6 : Micrographs of (a) eutectic surrounding the primary carbides (SEM) and (b) primary austenite dendrites (Optical at ×200)

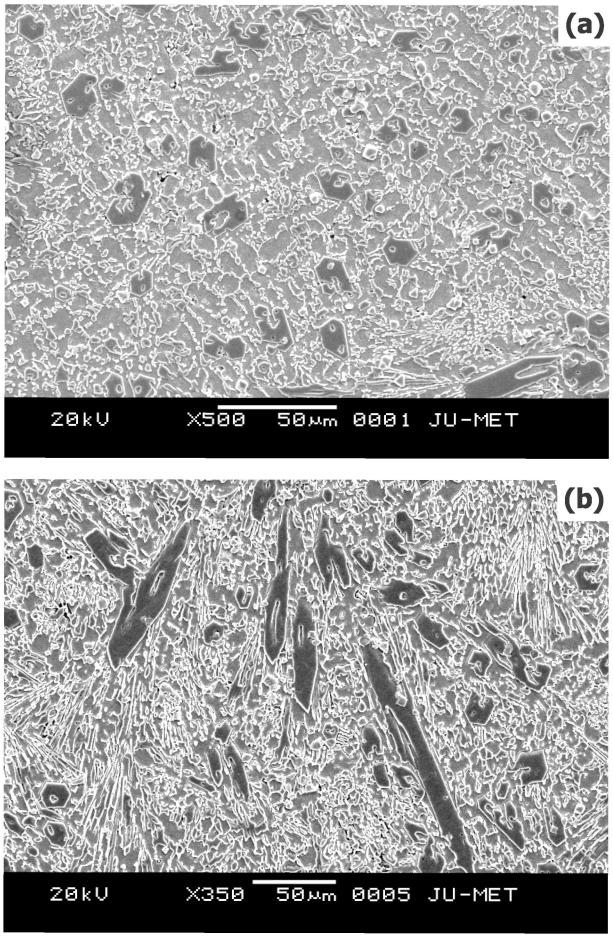

Fig. 7: SEM microstructure of hardfaced deposits (a) D1 and (b) D3 shows niobium and chromium carbides in the austenitic matrix

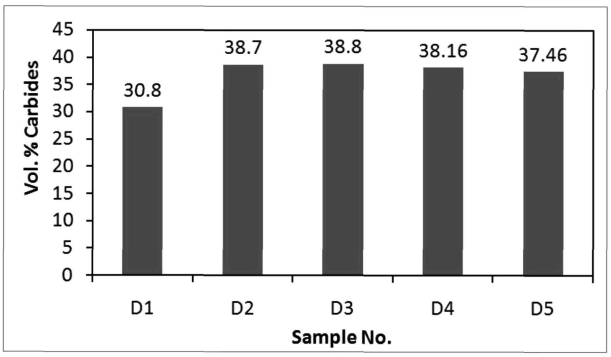

Fig. 9 : Volume fraction of carbide presents in different hardfaced deposits

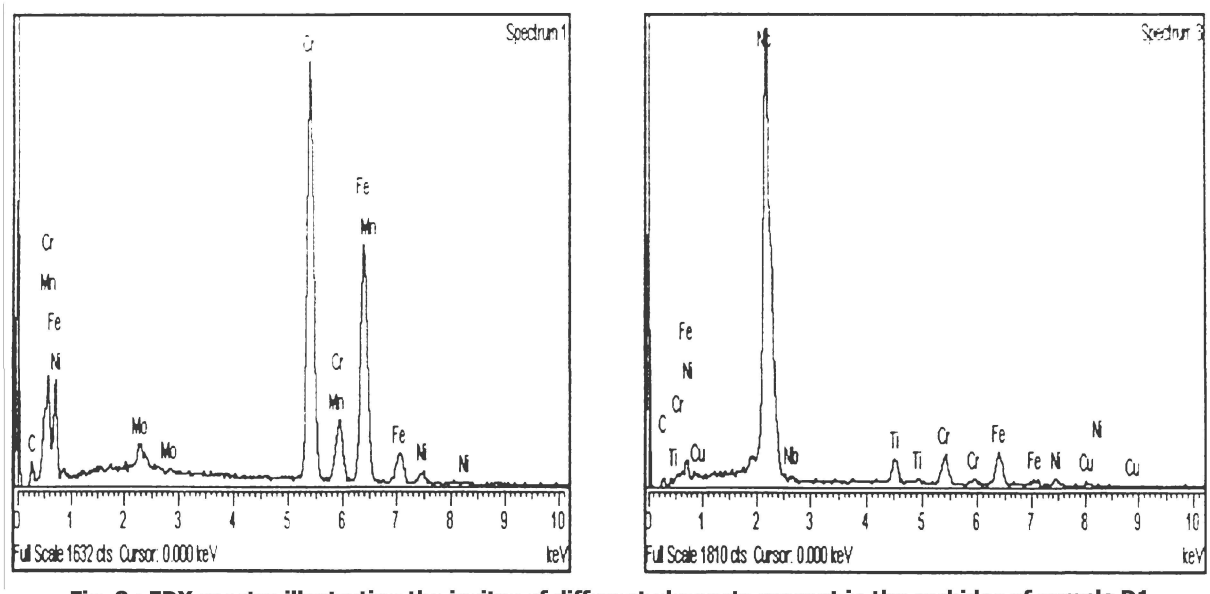

Fig. 8 : EDX spectra illustrating the incites of different elements present in the carbides of sample D1

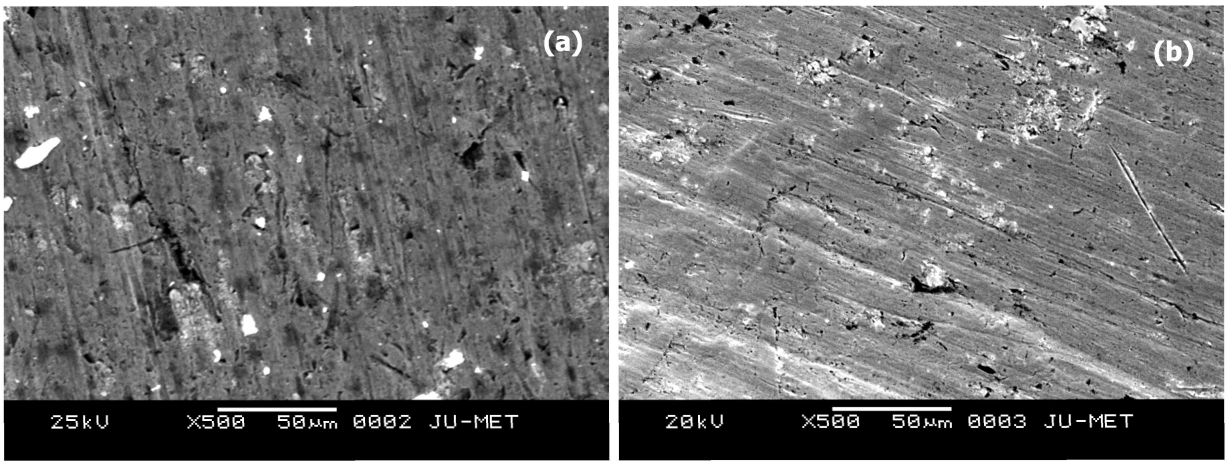

Fig. 10 : Scanning electron micrographs of different worn samples (a) D3 and (b) D5

4.0 CONCLUSIONS

The following conclusions may be drawn from this study:

1. Bond strength as evaluated by the shear strength between substrate cast iron and buffer/hardfacing layer is affected by the type buffer electrode used. High bond strength was obtained with buffer electrode containing higher Ni.
2. Improved low stress abrasive wear resistance of hardfacing deposits was obtained with relatively lower Ni containing buffer electrode.
3. Both bond strength and wear resistance are controlled by the microstructure developed with different types of buffer electrodes and a hardfacing electrode.
4. High wear resistance along with reasonably good bond strength of weld deposits on cast iron could be obtained even with buffer layer containing relatively lower Ni content (~36.5%).

REFERENCE

1. S. Chatterjee, and T. K. Pal: Wear, vol. 255, 2003, pp: 417-425.
2. R. Menon: Welding J., vol. 75, 1996, pp: 43–49.
3. Y. L. Su, and K. Y. Chen: Wear, vol. 209, 1997, pp: 160–170.
4. J. F. Knott, S. R. Valluri, D. M. R. Taplin, P. Rama Rao,

J. F. Knott, and R. Dubey, (Eds.): Proceedings of the 6th International Conference on Fracture (ICF 6), New Delhi, Pergamon Press, 1984, pp. 83–103.

5. C. A. Hippsley, and S. G. Druce: Acta Metall, Vol. 31, 1983, pp: 1861.
6. R. S. Jackson: JISI, 1970, vol.163-167, pp. 2003.
7. H. Berns and A. Fischer: Wear, 1987, pp. 401-429.
8. H. Fujimura, A. Notomi, Y. Kamito and N. Kinoshita: IIW Doc. XII-1071-88.
9. H. X. Chen, Z. C. Chang, J. C. Lu and H. T. Lin: Wear, 1993, vol.166, pp.197-201.
10. Metal Handbook, vol. 6, 9th ed., ASM International, Materials Park, OH, 1983, pp: 777.
11. S. Nagakura and S. Oketani: Trans. ISIJ, 1968, vol.8, pp.265-294.
12. W. R. Thorpe: Met. Forum, 1980, vol. 1, pp.62-73.
13. C. Y. Kung and J. J. Rayment: Metall. Trans., 1982, 13A, pp.328-331.
14. I. R. Sare: Met. Technol., 1979, vol.6, pp.412-419.
15. J. K. Fulcher, T. H. Kosel and N. F. Fiore: Wear, 1983, vol.84, pp.313-325.
16. K. H. Zum Gahr and D. V. Doane: Metall. Trans., 1980, vol.11A, pp. 613-620.
17. L. Xu. C. Vosf and D. St. John: Wear, 1993, vol. 162-164, pp. 820-832.
18. R. W. Durman: Foundry Trade J., 1973, vol.134, pp.645-651.
19. J.T.H. Pearce: Tnans. AFS, 1984, vol.92, pp.599-622.
20. R.S. Jackson: Br. Foundryman, 1974, vol.67, pp.34-41.
21. G. Laird. II: Trans. AFS, 1993, vol.101, pp.497-504.
22. ASTM A532-87, "standard specification for abrasion-resistant cast iron", Philadelphia, PA, ASTM.
23. AS2027-84, "Iron castings-abrasion-resisntant white iron", 1985, North Sydney, NSW, Standards Association of Australia.
24. G. Laird. II: Trans. AFS, 1991, vol.99, pp.339-357.
25. T. E. Norman, A. Solomon and D.V. Doane: Trans.AFS, 1959, vol.67, pp.242-256.
26. R. B. Jundlach: Trans. AFS, 1974, vol.82, pp.309-316.